

Optical Studies of Graphene Oxide/poly(amidoamine) Dendrimer Composite Thin Film and Its Potential for Sensing Hg^{2+} Using Surface Plasmon Resonance Spectroscopy

Mohammad Danial Aizad Roshidi,¹ Yap Wing Fen,^{1,2*} Nur Alia Sheh Omar,¹
Silvan Saleviter,¹ and Wan Mohd Ebtisyam Mustaqim Mohd Daniyal¹

¹Functional Devices Laboratory, Institute of Advanced Technology, Universiti Putra Malaysia,
43400 UPM Serdang, Selangor, Malaysia

²Department of Physics, Faculty of Science, Universiti Putra Malaysia,
43400 UPM Serdang, Selangor, Malaysia

(Received September 28, 2018; accepted October 31, 2018)

Keywords: surface plasmon resonance, optical properties, graphene oxide, poly(amidoamine) dendrimer

In this study, a graphene oxide/poly(amidoamine) (GO/PAMAM) dendrimer composite thin film was developed for the potential detection of Hg^{2+} using surface plasmon resonance (SPR) spectroscopy. Fourier transform infrared spectroscopy (FTIR) analysis proved the presence of amino, carboxylic acid, carboxyl, and hydroxyl groups in the GO/PAMAM thin film. The optical properties of the thin film were characterized using UV-Vis absorption spectroscopy. The UV-Vis analysis showed that the absorption of the GO/PAMAM thin film was high with an optical band gap of 4.01 eV. The incorporation of the GO/PAMAM thin film with SPR spectroscopy produced positive responses towards various Hg^{2+} concentrations. Atomic force microscopy results indicated that the thin film has an irregular edge and hence proved the interaction of mercury ions with the thin film.

1. Introduction

Graphene oxide (GO) has been under the spotlight in sensing application owing to its impressive chemical and physical properties.^(1–3) GO is the powerful oxidation product of graphite that contains multifunctional groups such as carboxyl, epoxy, ketone, and hydroxyl groups in its basal and edge planes.^(4,5) Furthermore, GO is said to be a “precise and ultrafast” transport medium for the selective permeation of ions and molecules in aqueous solutions.^(6,7) However, the limitation of using GO as a standalone material for sensing application is that it lacks absorption selectivity to the target absorbate. One of the alternative ways to improve the absorption selectivity is by combining GO with a dendrimer as a composite material.^(8–11)

Dendrimers are highly branched globular structures ranging from 2 to 20 in size; they are highly reactive because of the presence of a large number of terminal functional groups.^(12–14) They become favorite synthetic macromolecules in the field of biosensor technology, owing to their extraordinary structural properties such as monodispersity, controllable size and

*Corresponding author: e-mail: yapwingfen@gmail.com
<https://doi.org/10.18494/SAM.2019.2142>

structure, modifiable surface functionalities, hydrophilicity, and high mechanical and chemical stabilities.^(13,15,16) Poly(amidoamine) (PAMAM) dendrimers are preferable among the dendrimers for catalytic applications because of their regular structure and chemical versatility, possessing intrinsic amino and amido functionalities.⁽¹⁷⁾ The importance of using a dendrimer is to modify sensors with high stability, good reproducibility and repeatability, and low limit of detection.⁽¹³⁾

Surface plasmon resonance (SPR) is an optical process in which light satisfying a resonance condition excites a charge density wave propagating along the interface between a metal and a dielectric material by monochromatic and p-polarized light beams.^(18–20) This phenomenon is called surface plasmon resonance where the intensity of the reflected light is reduced at a specific incident angle producing a sharp shadow due to the resonance occurring between the incident beam and the surface plasmon wave.⁽²¹⁾ Since the last decade, SPR sensing has been receiving continuously growing attention from the scientific community owing to its advantages of real-time monitoring, label-free form, simple preparation, and remarkable sensitivity.^(22–24) In addition, SPR is a versatile technique used in sensing applications such as biosensors and material sensors.^(20,21,23) Previous research studies mainly focused on modifying gold films, which are required for the SPR phenomenon, to increase the sensitivity of the SPR sensor.^(25–28) However, to the best of our knowledge, SPR is yet to be applied with gold–GO/PAMAM composite thin films for heavy metal ion detection.

In this study, the structural and optical properties of a GO/PAMAM composite thin film were reported and the potential of thin film integration with SPR spectroscopy for sensing Hg^{2+} was explored.

2. Materials and Methods

2.1 Reagents and materials

GO (4 mg/mL) was purchased from Graphenea (Cambridge, MA, USA). PAMAM dendrimer, ethylenediamine generation 4.0 solution was purchased from Aldrich (USA).

2.2 Preparation of chemical

All chemicals used were of analytical grade and all solutions were prepared by using deionized water. A stock of 4 mg/mL GO was diluted with deionized water to decrease the concentration to 2 mg/mL. The PAMAM dendrimer was diluted with deionized water. Then, GO/PAMAM solution was produced by one-step self-assembly.⁽²⁹⁾ 0.5 mL of PAMAM water solution was added dropwise into 5.5 mL of GO solution with stirring for about 30 s to obtain the GO/PAMAM solution. Subsequently, a mercury standard solution with a concentration of 1000 ppm was diluted using the dilution formula $M_1V_1 = M_2V_2$ to produce Hg^{2+} solutions with concentrations of 0.5, 1, 5, 10, 20, 40, 60, 80, and 100 ppm.⁽³⁰⁾

2.3 Preparation of thin film

Glass cover slips ($24 \times 24 \times 0.1 \text{ mm}^3$, Menzel-Glaser, Germany) were cleaned with acetone to remove dirt from the glass slide surface before any coating process. The glass slide was first deposited with a thin gold layer using an SC7640 sputter coater. Then, spin coating (Specialty Coating System, P-6708D) was performed to produce a GO/PAMAM thin film layer on top of the gold layer. Approximately 1 ml of the solution was placed on the glass cover slip covering the majority of the glass surface. The glass cover slip was spun at 6000 revolutions per minute (rpm) for 30 s to produce the thin film.

2.4 Instrumental

The Fourier transform infrared spectroscopy (FTIR) test was carried out using a Thermo Nicolet Nexus 47 FTIR spectrometer with a wavelength range of $400\text{--}4000 \text{ cm}^{-1}$. UV-Vis-NIR spectroscopy (UV-3600 Shimadzu) was used to determine the absorbance of the samples in the range of 200 to 800 nm. Bruker AFM multimode 8 in the Scan Asyst mode was used to investigate the topography and height of the GO/PAMAM thin film in the range of $5 \times 5 \text{ }\mu\text{m}^2$.

2.5 Sensing metal ion

SPR spectroscopy was performed on the basis of the schematic diagram of the SPR instrument setup shown in Fig. 1 to test the capabilities of the thin film for sensing mercury ions.⁽³¹⁾ The SPR instrument was setup to measure the reflected He-Ne laser beam (632.8 nm , 5 mW) as a function of incident angle. The optical setup consists of a He-Ne laser, an optical stage driven by a stepper motor with a resolution of 0.001° (Newport MM 3000), a light attenuator, a polarizer, and an optical chopper (SR 540). The reflected He-Ne beam laser was detected by a sensitive photodiode and then processed with a lock-in-amplifier (SR 530).^(32–36)

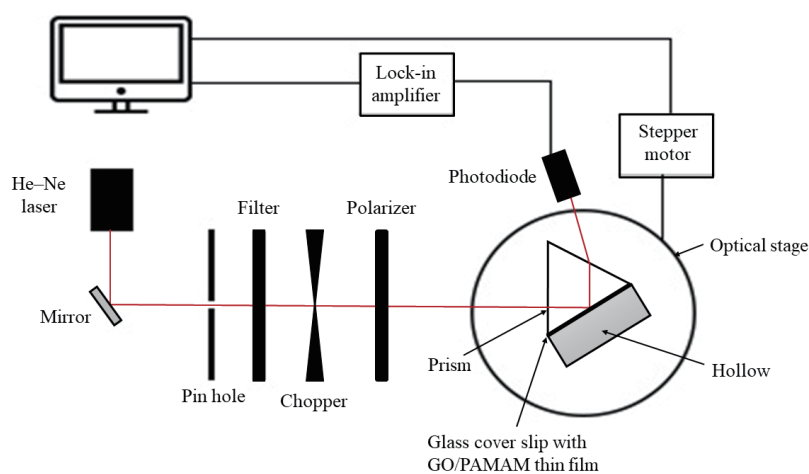


Fig. 1. (Color online) Experimental setup for angle scan SPR technique.

3. Results and Discussion

3.1 FTIR analysis

FTIR spectroscopy was carried out to analyze the functional group and interaction between GO and PAMAM. The FTIR spectra of GO, PAMAM, and GO/PAMAM composite thin films are shown in Fig. 2.

The GO spectrum depicts characteristic absorption bands at 3313.43 and 1432.82 cm^{-1} , which are attributed to the O–H group from the carboxyl group.^(29,37) Furthermore, the weaker band at 2895.71 cm^{-1} is attributed to the presence of the carboxylic acid COOH.⁽³⁸⁾ Next, the bands at 1122.75 and 1661.52 cm^{-1} correspond to the C–O stretching vibrations of the carbonyl and C=C groups, respectively.⁽²⁹⁾

PAMAM exhibits two adsorption bands at 1654.14 and 1466.70 cm^{-1} , which are C=C in the presence of the carboxyl group in the polymer chain and the amide stretching group C(O)–NH, respectively.⁽²⁹⁾ The bands at 3329.05 and 1126.67 cm^{-1} could be assigned to the amine stretching group of the polymers, N–H.^(29,38)

Lastly, all the GO/PAMAM bands have nearly the same characteristic peaks of GO and PAMAM. However, there are small differences observed by closely examining the FTIR band of GO/PAMAM. It was observed that the FTIR bands at 1000 to 1400 cm^{-1} slightly shifted, indicating the interaction of GO and PAMAM. Moreover, the hydroxyl group O–H was eliminated and replaced with N–H at a peak of around 1430 to 1470 cm^{-1} . This peak shows evidence of a successful reaction.^(11,8)

3.2 Optical studies

Optical properties were measured by using the absorbance spectrum of the thin film with a wavelength range of 220 to 800 nm. The absorbance curves of GO/PAMAM are shown in

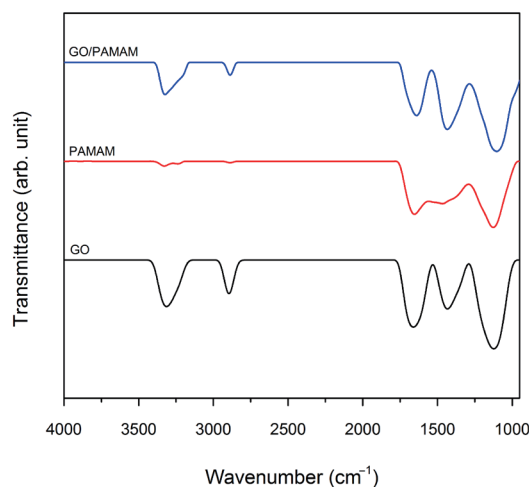


Fig. 2. (Color online) FTIR spectra of GO, PAMAM, and GO/PAMAM composite thin films.

Fig. 3. From the graph, the maximum absorption wavelength can be determined to range from 278 to 285 nm. The absorption peaks at the shoulder approaching 303 nm can be assigned to $n-\pi^*$ transitions of C=O.⁽³⁹⁾ The absorbance A of the sample depends on the ratio intensity of illumination on the detector in the absence (I_o) and presence (I_t) of the sample.

$$A = \log_{10} \frac{I_o}{I_t} \quad (1)$$

Another quantity that can be measured is the absorbance coefficient, which is a useful quantity when comparing samples of various thicknesses. The absorbance coefficient is given as

$$\alpha = 2.303 \frac{A}{t}, \quad (2)$$

where t is the thickness of the sample and α is the absorbance coefficient. To calculate the optical band gap energy from absorption spectra, the Tauc relation is used,

$$\alpha = \frac{k(h\nu - E_g)^{1/2}}{h\nu}. \quad (3)$$

By rearranging the above equation,

$$(\alpha h\nu)^2 = k(h\nu - E_g), \quad (4)$$

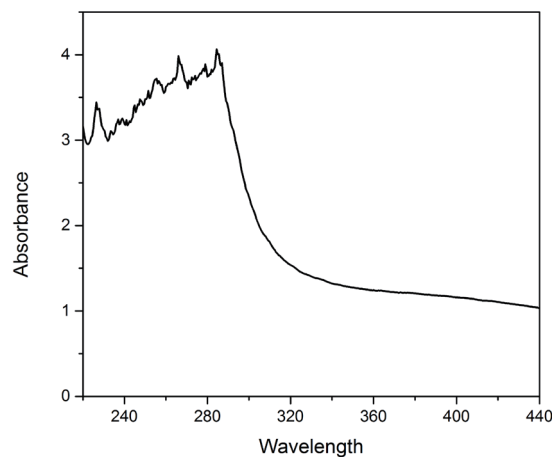


Fig. 3. Absorbance curves of GO/PAMAM.

where $h\nu$ is the photon energy, h is Plank's constant, α is the absorption coefficient, E_g is the optical energy band gap, and k is a constant; for direct transitions, $n = \frac{1}{2}$.⁽⁴⁰⁾ When $(\alpha h\nu)^2$ is plotted against $h\nu$, the intersection of this straight line on the x-axis gives the optical band gap E_g .⁽⁴¹⁾ The graph of $(\alpha h\nu)^2$ versus $h\nu$ for the GO/PAMAM thin film is shown in Fig. 4, which gives the energy band gap E_g of 4.01 eV.

3.3 Sensing properties

A preliminary SPR test was carried out with deionized water in contact with a gold–GO/PAMAM layer. The deionized water was injected into the cell in contact with the gold–GO/PAMAM layer film. The SPR reflectivity curve for the gold–GO/PAMAM layer film in contact with deionized water is shown in Fig. 5 and the resonance angle obtained is 53.94°. Then, the SPR experiment was carried out using a different Hg^{2+} concentration in an aqueous solution that was injected into the cell attached to the composite layer. The SPR reflectivity curves for Hg^{2+} concentrations ranging from 0.1 to 80 ppm in contact with the gold–GO/PAMAM layer are shown in Fig. 6. The resonance angles determined from the SPR curves are 53.853, 53.881, 53.842, 53.839, 53.824, and 53.809° for 1, 5, 10, 20, 40, and 60 ppm, respectively. This may be determined from the slight shift of the resonance angle with increasing Hg^{2+} concentration. From the results, the resonance angle shifted to the left owing to changes in thickness and refractive index.⁽⁴²⁾

According to our previous reports,^(1,6,11,12) we believe that the GO/PAMAM structure plays a vital role in adsorbing Hg^{2+} . GO/PAMAM have high stability constant values with Hg^{2+} owing to a carboxylic group in GO and an amine group in PAMAM.⁽⁴³⁾ The schematic diagram of a possible connection of Hg^{2+} to GO/PAMAM is shown in Fig. 7.

The shift in resonance angle ($\Delta\theta$) has been introduced as a parameter to measure the sensitivity of a sensor.⁽⁴⁴⁾ It is determined by taking the difference between the resonance

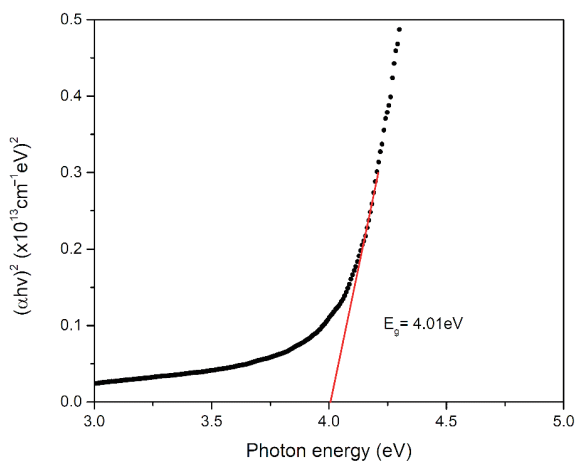


Fig. 4. (Color online) Energy band gap of GO/PAMAM.

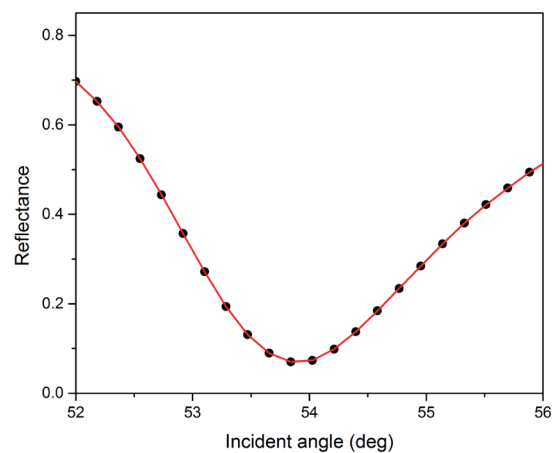


Fig. 5. (Color online) SPR curve of gold–GO/PAMAM thin film in contact with deionized water.

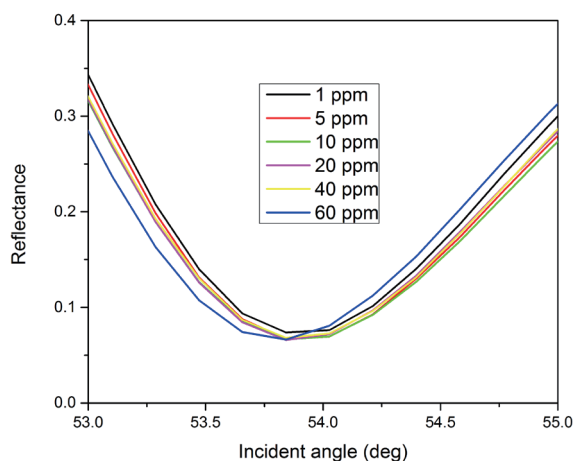


Fig. 6. (Color online) SPR reflectivity curves for Hg^{2+} concentrations ranging from 0.1 to 80 ppm in contact with gold-GO/PAMAM layer.

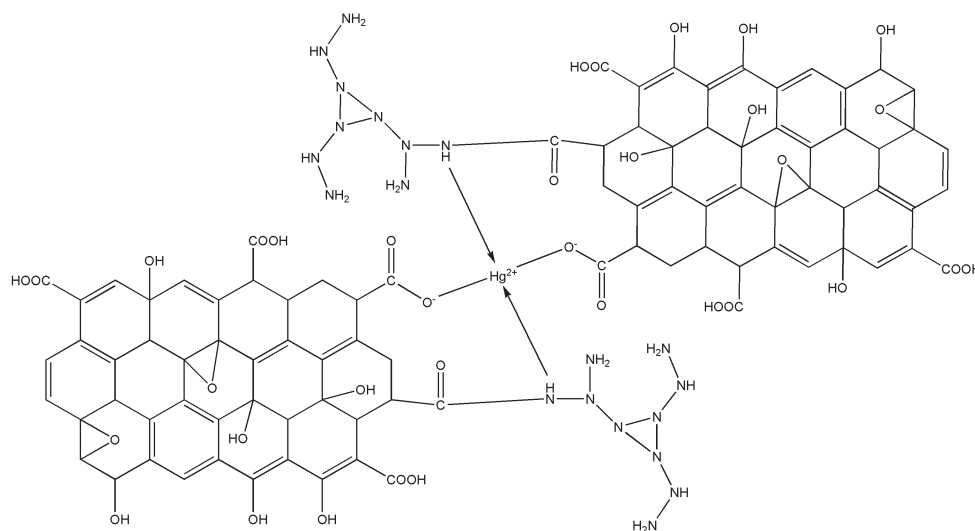


Fig. 7. Possible sensing mechanism of GO/PAMAM with Hg^{2+} .

angles of the sample and deionized water as references. The relationship between $\Delta\theta$ and the Hg^{2+} concentration is shown in Fig. 8. The linear regression analysis of the optical sensor is based on the GO/PAMAM thin film for Hg^{2+} with a sensitivity of $0.00657^\circ \text{ppm}^{-1}$ for a lower concentration (below 10 ppm) and a sensitivity of $0.00068^\circ \text{ppm}^{-1}$ for a higher concentration (above 10 ppm).

3.4 Surface morphology

The topography of a thin film sample has been determined using AFM, which resolves the visualization of a substance that is impossible to see by the naked eye. The AFM images were normally taken at the center of the drop, where the particles are well scattered and

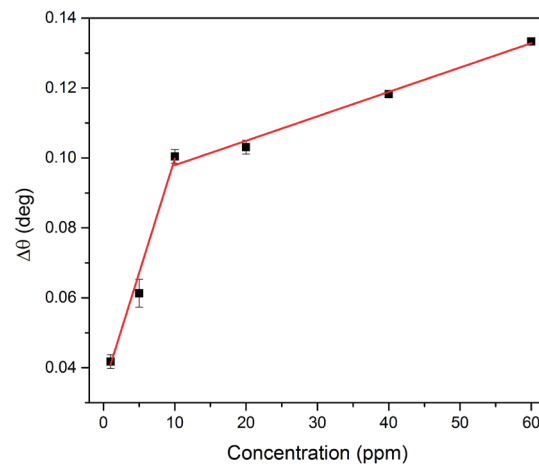


Fig. 8. (Color online) Shift in resonance angle for different concentrations of Hg^{2+} in contact with gold-GO/PAMAM.

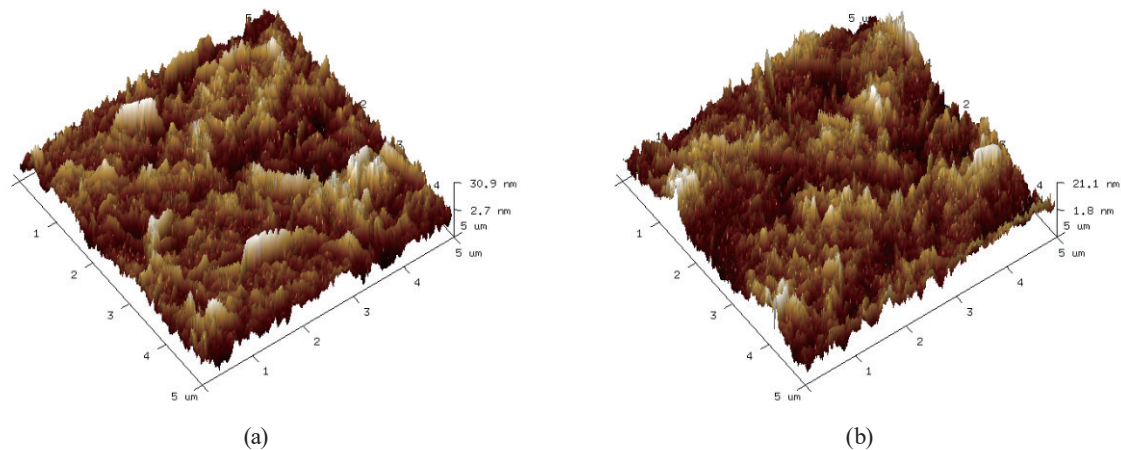


Fig. 9. (Color online) GO/PAMAM thin film (a) before and (b) after adding Hg^{2+} with a concentration of 40 ppm.

detached. The AFM images show the topography of the thin film shown in Fig. 9(a). The topography can be determined by measuring the root-mean-square (RMS) roughness, which represents the relative roughness of a surface and the standard deviation of the surface height.⁽⁴⁵⁾ GO/PAMAM has an irregular edge with an RMS of 7.79 nm. After adding Hg^{2+} with a concentration of 40 ppm, the RMS decreases to 5.49 nm as shown in Fig. 9(b).

4. Conclusion

In this research, a GO/PAMAM thin film was successfully prepared by spin coating. The FTIR result confirmed the interaction between GO and PAMAM, which has a peak at around 1430 to 1470 cm^{-1} , and that O–H was eliminated and replaced with N–H. The UV-Vis absorption of the GO/PAMAM thin film was low with an optical band gap of 4.01 eV. The incorporation of the GO/PAMAM thin film with surface plasmon resonance spectroscopy

produced positive responses towards the Hg^{2+} ion solutions with a sensitivity of $0.00657^\circ \text{ppm}^{-1}$ for a lower concentration (below 10 ppm) or a sensitivity of $0.00068^\circ \text{ppm}^{-1}$ for a higher concentration (above 10 ppm). AFM confirmed that the GO/PAMAM thin film has an irregular edge and that RMS decreases when Hg^{2+} is added to the thin film.

Acknowledgments

The authors gratefully acknowledge Universiti Putra Malaysia (UPM) for the financial support of this study through Putra Grant. They also acknowledge the Department of Physics and Institute of Advanced Technology, Universiti Putra Malaysia, for providing laboratory facilities.

References

- 1 K. Jayakumar, R. Rajesh, V. Dharuman, R. Venkatesan, J. H. Hahn, and S. K. Pandian: *Biosens. Bioelectron.* **31** (2012) 406. <https://doi.org/10.1016/j.bios.2011.11.001>
- 2 T. Yan, H. Zhang, D. Huang, S. Feng, M. Fujita, and X. Gao: *Nanomaterials* **7** (2017) 59. <https://doi.org/10.3390/nano7030059>
- 3 S. Stankovich, D. A. Dikin, R. D. Piner, K. A. Kohlhaas, A. Kleinhammes, Y. Jia, Y. Wu, S. T. Nguyen, and R. S. Ruoff: *Carbon* **4** (2017) 1558. <https://doi.org/10.1016/j.carbon.2007.02.034>
- 4 M. H. M. Zaid, J. Abdullah, N. A. Yusof, Y. Sulaiman, H. Wasoh, M. F. M. Noh, and R. Issa: *Sens. Actuators, B* **241** (2017) 1024. <https://doi.org/10.1016/j.snb.2016.10.045>
- 5 O. C. Compton and S. T. Nguyen: *Small* **6** (2010) 711. <https://doi.org/10.1002/sml.200901934>
- 6 W. M. E. M. M. Daniyal, Y. W. Fen, J. Abdullah, S. Saleviter, and N. A. S. Omar: *Optik* **173** (2018) 71. <https://doi.org/10.1016/j.ijleo.2018.08.014>
- 7 R. K. Joshi, P. Carbone, F. C. Wang, V. G. Kravets, Y. Su, I. V. Grigorieva, H. A. Wu, A. K. Geim, and R. R. Nair: *Science* **343** (2014) 752. <https://doi.org/10.1126/science.1245711>
- 8 M. Nonahal, H. Rastin, M. R. Saeb, M. G. Sari, M. H. Moghadam, P. Zarrintaj, and B. Ramezanzadeh: *Prog. Org. Coat.* **114** (2018) 233. <https://doi.org/10.1016/j.porgcoat.2017.11.016>
- 9 B. Pan, F. Gao, and H. Gu: *J. Colloid Interface Sci.* **284** (2005) 1. <https://doi.org/10.1016/j.jcis.2004.09.073>
- 10 X. Shi, S. H. Wang, M. Shen, M. E. Antwerp, X. Chen, C. Li, E. J. Petersen, Q. Huang, W. J. Weber, and J. R. Baker: *Biomacromolecules* **10** (2009) 1744. <https://doi.org/10.1021/bm9001624>
- 11 Y. Yuan, G. Zhang, Y. Li, G. Zhang, F. Zhang, and X. Fan: *Polym. Chem.* **4** (2013) 2164. <https://doi.org/10.1039/c3py21128b>
- 12 E. B. Bahadir and M. K. Sezgin: *Talanta* **148** (2016) 427. <https://doi.org/10.1016/j.talanta.2015.11.022>
- 13 F. Zhang, B. Wang, S. He, and R. Man: *J. Chem. Eng. Data* **59** (2014) 1719. <https://pubs.acs.org/doi/abs/10.1021/je500219e>
- 14 M. Hasanzadeh, N. Shadjou, M. Eskandani, J. Soleymani, F. Jafari, and M. D. L. Guardia: *TrAC, Trends Anal. Chem.* **53** (2014) 137. <https://doi.org/10.1016/j.trac.2013.09.015>
- 15 A. Bosnjakovic: Ph.D. Dissertation, Wayne State University, Michigan (2011) p. 1.
- 16 R. Rajesh, S. S. Kumar, and R. Venkatesan: *New J. Chem.* **38** (2014) 1551. <https://doi.org/10.1039/c3nj01050c>
- 17 N. T. P. Azar, P. Mutlu, R. Khodadust, and U. Gunduz: *Hacettepe Biol. Chem.* **41** (2013) 289. http://www.hjbc.hacettepe.edu.tr/site/assets/files/1789/41-3_a13.pdf
- 18 J. Homola: *Sens. Actuators, B* **41** (1997) 207. [https://doi.org/10.1016/S0925-4005\(97\)80297-3](https://doi.org/10.1016/S0925-4005(97)80297-3)
- 19 J. Homola and S. Yee: *Sens. Actuators, B* **37** (1996) 145. [https://doi.org/10.1016/S0925-4005\(97\)80130-X](https://doi.org/10.1016/S0925-4005(97)80130-X)
- 20 W. M. E. M. M. Daniyal, S. Saleviter, and Y. W. Fen: *Sens. Mater.* **30** (2018) 2023. <https://doi.org/10.18494/SAM.2018.1952>
- 21 Y. W. Fen, W. M. M. Yunus, and N. A. Yusof: *Sens. Actuators, B* **171** (2012) 287. <https://doi.org/10.1016/j.snb.2012.03.070>
- 22 S. B. D. Borah, T. Bora, S. Baruah, and J. Dutta: *Groundwater Sustainable Dev.* **1** (2015) 1. <https://doi.org/10.1016/j.gsd.2015.12.004>
- 23 J. Homola, S. S. Yee, and G. Gauglitz: *Sens. Actuators, B* **54** (1999) 3. [https://doi.org/10.1016/S0925-4005\(98\)00321-9](https://doi.org/10.1016/S0925-4005(98)00321-9)

- 24 D. R. Shankaran, K. V. Gobi, and N. Miura: *Sens. Actuators, B* **121** (2007) 158. <https://doi.org/10.1016/j.snb.2006.09.014>
- 25 Y. W. Fen, W. M. M. Yunus, Z. A. Talib, and N. A. Yusof: *Spectrochim. Acta A Mol. Biomol. Spectrosc.* **134** (2015) 48. <https://doi.org/10.1016/j.saa.2014.06.081>
- 26 Y. W. Fen, W. M. M. Yunus, N. A. Yusof, N. S. Ishak, N. A. S. Omar, and A. A. Zainudin: *Optik* **126** (2015) 4688. <https://doi.org/10.1016/j.ijleo.2015.08.098>
- 27 Y. W. Fen, W. M. M. Yunus, and Z. A. Talib: *Sens. Mater.* **25** (2013) 99. <https://doi.org/10.18494/SAM.2013.797>
- 28 A. A. Zainudin, Y. W. Fen, N. A. Yusof, S. H. Al-Rekabi, M. A. Mahdi, and N. A. S. Omar: *Spectrochim. Acta A Mol. Biomol. Spectrosc.* **191** (2018) 111. <https://doi.org/10.1016/j.saa.2017.10.013>
- 29 Y. Piao, T. Wu, and B. Chen: *Ind. Eng. Chem. Res.* **55** (2016) 6113. <https://doi.org/10.1021/acs.iecr.6b00947>
- 30 Y. W. Fen, W. M. M. Yunus, and N. A. Yusof: *Sens. Mater.* **23** (2011) 325. <https://doi.org/10.18494/SAM.2011.723>
- 31 A. A. Zainudin, Y. W. Fen, N. A. Yusof, and N. A. S. Omar: *Optik* **144** (2017) 308. <https://doi.org/10.1016/j.ijleo.2017.07.001>
- 32 Y. W. Fen, W. M. M. Yunus, and N. A. Yusof: *Sens. Actuators, B* **171** (2012) 287. <https://doi.org/10.1016/j.snb.2012.03.070>
- 33 N. A. S. Omar, Y. W. Fen, J. Abdullah, C. E. N. C. E. Chik, and M. A. Mahdi: *Sens. Bio-Sens. Res.* **20** (2018) 16. <https://doi.org/10.1016/j.sbsr.2018.06.001>
- 34 N. A. S. Omar and Y. W. Fen: *Sens. Rev.* **38** (2018) 106. <https://doi.org/10.1108/SR-07-2017-0130>
- 35 S. Saleviter, Y. W. Fen, N. A. S. Omar, A. A. Zainudin, and N. A. Yusof: *Sens. Lett.* **15** (2017) 862. <https://doi.org/10.1166/sl.2017.3883>
- 36 S. Saleviter, Y. W. Fen, N. A. S. Omar, A. A. Zainudin, and W. M. E. M. M. Daniyal: *Result Phys.* **11** (2018) 188. <https://doi.org/10.1016/j.rinp.2018.08.040>
- 37 S. Liu, J. Yan, G. He, D. Zhong, J. Chen, L. Shi, X. Zhou, and H. Jiang: *J. Electroanal. Chem.* **672** (2012) 40. <https://doi.org/10.1016/j.jelechem.2012.03.007>
- 38 D. L. Pavia, G. M. Lampman, G. S. Kriz, and J. R. Vyvyan: *Introduction to Spectroscopy* (Cengage Learning Asia, Singapore, 2015).
- 39 Z. Luo, L. Yuwen, H. Yujie, J. Tian, X. Zhu, L. Weng, and L. Wang: *Biosens. Bioelectron.* **36** (2012) 179. <https://doi.org/10.1016/j.bios.2012.04.009>
- 40 J. Tauc, R. Grigorovici, and A. Vancu: *Phys. Status Solidi B* **15** (1966) 627. <https://doi.org/10.1002/pssb.19660150224>
- 41 H. Abdulla and A. Abbo: *Int. J. Electrochem. Sci.* **7** (2012) 10666. <http://www.electrochemsci.org/papers/vol7/71110666.pdf>
- 42 Y. W. Fen, W. M. M. Yunus, and Z. A. Talib: *Optik* **124** (2013) 126. <https://doi.org/10.1016/j.ijleo.2011.11.035>
- 43 B. B. Tewari: *Rev. Soc. Quím. Perú* **77** (2011) 144. <http://www.scielo.org.pe/pdf/rsqp/v77n2/a07v77n2.pdf>
- 44 M. M. Abdi, L. C. Abdullah, A. R. Sadrolhosseini, W. M. M. Yunus, M. M. Moksini, and P. M. Tahir: *PLOS ONE* **6** (2011) e24578. <https://doi.org/10.1371/journal.pone.0024578>
- 45 A. W. Mohammad, N. Hilal, L. Y. Pei, M. I. N. H. Amin, and R. Raslan: *Sains Malays.* **40** (2011) 237. <http://journalarticle.ukm.my/704/>